Recombinant immunotoxin engineered for low immunogenicity and antigenicity by identifying and silencing human B-cell epitopes

Wenhai Liu[1], Masanori Onda[1,2], Byungkook Lee, Robert J. Kreitman, Raffit Hassan, Laiman Xiang, and Ira Pastan[2]

Laboratory of Molecular Biology, Center for Cancer Research, National Cancer Institute, National Institutes of Health, Bethesda, MD 20892

Recombinant immunotoxins (RITs) are hybrid proteins used to treat cancer. These proteins are composed of an Fv that reacts with cancer cells joined to a portion of *Pseudomonas* exotoxin A, which kills the cell. Because the toxin is a foreign protein, it can induce neutralizing antibodies and thereby limit the number of doses a patient can receive. We previously identified seven major mouse B-cell epitopes in the toxin, and subsequently silenced them using point mutations that converted large hydrophilic amino acids to alanine, yet retained full antitumor activity. Here we present results in which we identify and silence human B-cell epitopes in the RIT HA22. We obtained B cells from patients with antibodies to RITs, isolated the corresponding variable fragments (Fvs), and constructed a phage-display library containing Fvs that bind to the RITs. We then used alanine scanning mutagenesis to locate the epitopes. We found that human and mouse epitopes frequently overlap but are not identical. Most mutations that remove mouse epitopes did not remove human epitopes. Using the epitope information, we constructed a variant immunotoxin, HA22-LR-LO10, which has low reactivity with human antisera, yet has high cytotoxic and antitumor activity and can be given to mice at high doses without excess toxicity. The toxin portion of this RIT (LR-LO10) can be used with Fvs targeting other cancer antigens and is suitable for clinical development.

cancer treatment | immunotherapy | leukemia | mesothelioma | protein engineering

Many mAbs have been developed for cancer treatment, but few of these are clinically useful as single agents because they do not efficiently kill those cells (1). Instead, antibodies of this type can be used as carriers for cytotoxic drugs, radio-isotopes, or protein toxins (2). Our laboratory has focused on using antibodies joined to *Pseudomonas* exotoxin A (PE) to kill cancer cells. We use recombinant DNA techniques to replace the cell-binding domain of the toxin with the variable fragment (Fv) of an antibody that reacts with an antigen on a cancer cell, generating chimeric proteins called recombinant immunotoxins (RITs). We are currently testing three RITs in patients, all of which contain a 38-kDa fragment of PE (composed of domain II and domain III, as shown in Fig. 1) connected to Fvs with three different specificities. One RIT under clinical evaluation is Moxetumomab pasudotox [also known as HA22 or anti-CD22 (Fv)-PE38], which targets CD22 expressed on B-cell malignancies (3). In a phase I trial it produced complete remissions in over 50% of patients with drug-resistant hairy cell leukemia (4) and has produced complete remissions in several patients with acute lymphoblastic leukemia (5). Another RIT undergoing clinical trials, LMB2 or anti–Tac(Fv)-PE38, has shown antitumor activity in patients with adult T-cell leukemia and other hematologic malignancies (6). A third RIT, SS1P or antimesothelin (Fv)-PE38, is being evaluated in pleural mesothelioma. This RIT has given a few minor responses when tested alone, but when combined with chemotherapy has produced many partial responses (7, 8).

One major factor that limits the efficacy of these RITs is that PE38 is a bacterial protein that can induce antibody responses in patients (2, 7). In patients with hematological malignancies, antibody formation either does not occur or is greatly delayed, because the immune system is suppressed by the disease or the chemotherapy used to treat the malignancy. Thus, many treatment cycles can usually be given to these patients (2). In contrast, in patients with solid tumors, such as mesothelioma, the immune system is intact and antibodies usually develop after three doses (one cycle) that neutralize the toxin and prevent effective retreatment (7, 8). Another factor that limits efficacy of various immunotoxins is the development of a capillary leak syndrome because of nonspecific damage to the endothelial cells by high concentrations of immunotoxins in the blood (2, 7, 8).

We previously described the design and construction of the RIT HA22-LR-8M in which the mouse B-cell epitopes were identified and silenced by mutations (9). To do this, domain II of PE was deleted (except for the furin processing site) and eight point mutations were introduced into domain III to remove large hydrophilic residues (HA22-LR-8M in Fig. 1). HA22-LR-8M has excellent antitumor activity, yet does not induce the formation of antitoxin antibodies when injected repeatedly into mice, and does not induce a recall response in preimmunized mice (9). These results show that, using a mouse model, it is possible to produce an active nonimmunogenic RIT. In the present study our goal was to produce a RIT that is not immunogenic in humans by identifying and silencing human B-cell epitopes.

Results

Isolation and Sequence Determination of Human scFv Specific for PE38. We constructed six phage-display libraries of Fvs isolated from patients who had developed neutralizing antibodies to RITs (10, 11), and selected for those phage that bound specifically to PE38. Fig. 2 summarizes our strategy and Dataset S1 lists the characteristics of each library and the clones obtained. Each library was prepared from a single patient.

We obtained a combined total of 710 Fv-containing phage clones from the six libraries. Sequencing revealed that 103 of these clones had unique human heavy-chain and human κ–light-chain sequences, except for two clones with the same light-chain sequence (Datasets S2 and S3). To confirm that the phage Fvs bound to the toxin, we did competition studies and showed that immune antisera from patients blocked the binding of the phage
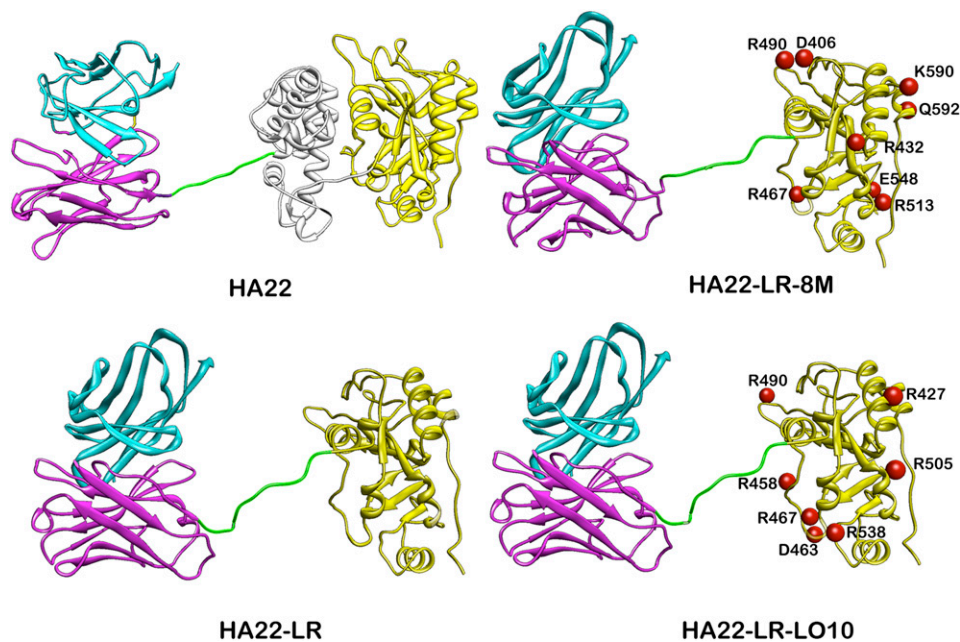
Fig. 1. Ribbon drawings of HA22, HA22-LR, HA22-LR-8M, and HA22-LR-LO10. The light chain is in cyan and the heavy chain is in magenta. Domain II is in gray and domain III in yellow. The linker between Fv and the toxin containing the furin site is green. The numbers on domain III indicate the mutated residues. The Fv was modeled using the heavy chain of the PDB structure 1hil and the light chain of 1fbi. The toxin part is from the PDB structure 1ikq. The linker conformation and length were chosen arbitrarily.

to the PE38 portion of LMB-9, a PE38-containing immunotoxin that binds to a different antigen (12). The strength of binding was then measured using an ICC-ELISA (13); 56 clones had strong binding and were used to determine the location of the human-specific epitopes in PE38. The other remaining 47 clones bound weakly and were discarded.

Location of Human B-Cell Epitopes. To identify phage that bind to domain III, we measured the binding of each clone to HA22-LR, a RIT from which most of domain II is deleted (Fig. 1). Fifteen of the 56 strongly binding phage did not react with HA22-LR, indicating that the epitopes recognized by these Fvs are located on domain II. We used the remaining 41 phage to identify the residues that make up the B-cell epitopes in domain III by measuring their binding to 36 different mutant proteins in which individual amino acids on the surface of domain III were

Fig. 2. Strategy for isolating phage-expressing Fvs reacting with PE38 from patient blood. 1, RNA was extracted from blood samples obtained from patients who had been treated with RITs. 2, The cDNAs encoding Fvs were synthesized and amplified by PCR. 3, The Fvs were displayed on phage. 4, The phage that contained Fvs reacting with the toxin (PE38) were isolated by panning on a biotinylated RIT that has PE38 attached to a different Fv (LMB-9) using streptavidin modified magnetic beads. 5, Phage were released from the beads using low pH and individual phage that bound to domain III were sequenced.

mutated from a large polar amino acid to alanine or glycine, as previously described (14, 15). The results are shown in Fig. 3, where very low binding is shown in black and normal reactivity in white. The results can be grouped into six human B-cell epitopes, in which a single mutation or nearby mutations decrease the binding of multiple phage to the same mutant protein.

Epitope H1 includes residues D403, E420, and R427 (Fig. 3). As expected for mutations that make up an epitope, these residues are spatially close together on the surface of domain III. Epitope H2 mainly includes D463, R467, and Y481, with minor contributions from several other nearby residues (Fig. 3). Epitope H3 consists of R458, and epitope H4 contains R505 and is recognized by 11 different phages. Epitope H5 includes R490 and R576. These residues are spatially adjacent even though separated by 86 amino acids in the sequence. Epitope H6 contains R563 and R538.

Comparison of Human- and Mouse-Specific B-Cell Epitopes. Fig. 4 shows the location of the mutations that eliminate human- and mouse-specific epitopes in PE38. Residues from human-specific epitopes are colored red, mouse-specific are green, and those included from both species are yellow. It is evident that some residues are important for both human and mouse antibody binding and others are specific for one or the other.

Epitope H1 contains D403, E420, R427, and E431. R427 and E431 are in mouse epitope 4a, and E420 in mouse epitope 7; these three residues are important for both mouse and human antibody binding. Epitope H2 contains residues R467 and D463, which are also in mouse epitope 2c, E548, which is in mouse epitope 6a, and D581 from mouse epitope 6b. Residues D461, Y481, L516, E522, and R551 are human-specific epitopes. Epitope H3 contains only R458, which is also in mouse epitope 4b. Epitope H4 contains R432 and R505. R432 is in mouse epitope 4a and R505 is a human-specific residue. Epitope H5 is composed of R490 and R576, which are both in mouse epitope 5. Human epitope H6 is composed of R538 and R563. R538 is in mouse epitope 2c and R563 in mouse epitope 4a.
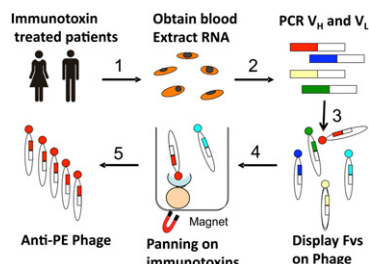
MEDICAL SCIENCES

Fig. 3. Reactivity of the Fv-phage with mutant domain III proteins in which bulky amino acids were mutated to alanine. Black cells indicate less than 10% of the reactivity compared with no mutation. White cells indicate greater than 10% reactivity, gray not tested. The mutants are ordered by their location from the N terminus to the C terminus. Each column indicates an individual phage and epitope groups are shown on the left.

Production of a Low Antigenic RIT for Humans. We used the information on the amino acid composition of each epitope to construct RITs with mutations that greatly reduced their reactivity with human antisera, yet maintained good cytotoxic and antitumor activities. HA22-LR-8M is a variant that has all mouse B-cell epitopes silenced by eight point mutations, yet is fully active (Fig. 1). Because residues R467 and R490 are common to mouse and human epitopes, they were included in the new mutant. We prepared HA22-LR-LO10 (Fig. 5A) by combining the two common mutations (R467 and R490) with five human-specific mutations (R427, R458, D463, R505, R538). The locations of the mutations are shown in Fig. 1; they are dispersed over the exposed surface of the protein.
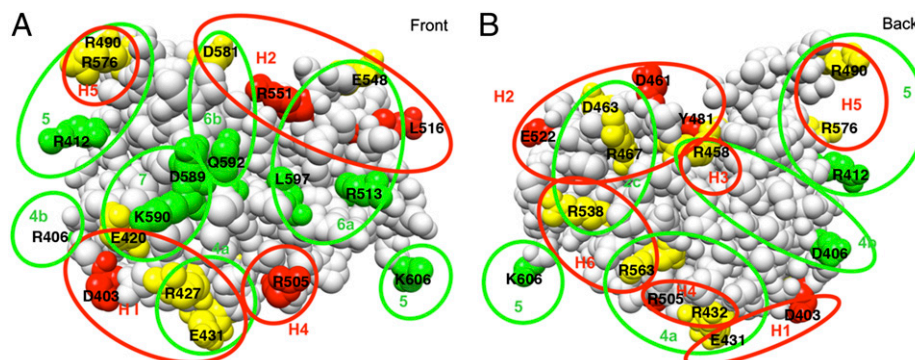
Fig. 4. Location of residues that define human and mouse B-cell eitopes in domain III. (A) Front view and (B) back view. The amino acids that when mutated decreased the binding of phage or mAbs are colored red (human specific epitopes), green (mouse specific epitopes), and yellow (shared epitopes between human and mouse). The proposed region encompassing each epitope is indicated with red circles (human epitopes: H1, H2, H3, H4, H5, and H6) and green circles (mouse epitopes: 2c, 4a, 4b, 5, 6a, 6b, and 7). The model of domain III was constructed by removing residues 1–394 from the crystal structure of native PE (PDB structure 1ikq).
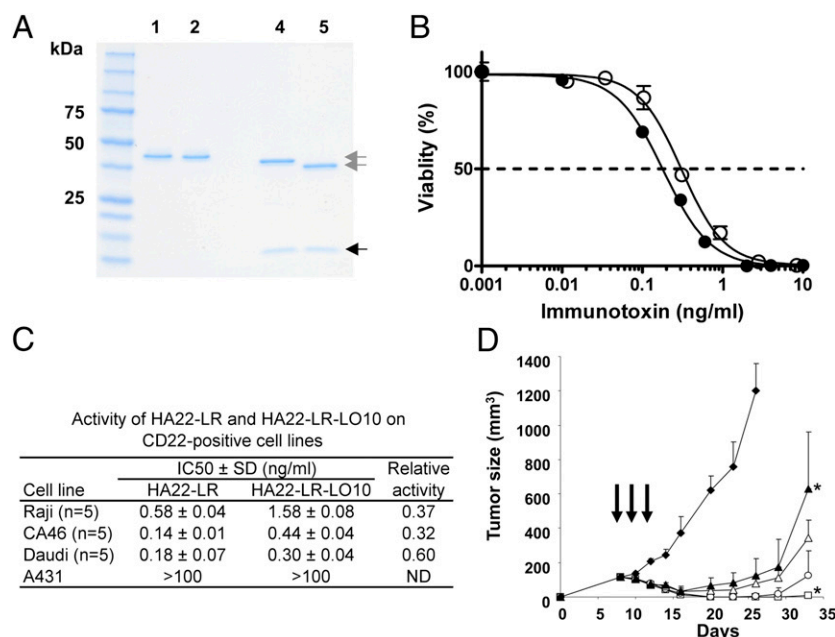
Fig. 5. Characterization and properties HA22-LR-LO10. (*A*) SDS PAGE gel of purified RITs. The purified proteins (2 μg) were analyzed on a 4–20% gradient SDS polyacrylamide gel under nonreducing conditions (lanes 1 and 2) and under reducing conditions (lanes 4 and 5). Lanes 1 and 4, HA22-LR; lanes 2 and 5, HA22-LR-LO10; molecular mass standards are indicated on the left; gray arrows, V_H-toxin; black arrow, V_L. (*B*) Cytotoxic activity of HA22-LR and HA22-LR-LO10 on Daudi cells. The cytotoxicity assays were performed at least five times using three values for each point. ●, HA22-LR; ○, HA22-LR-LO10. Data are expressed as the mean ± SD. (*C*) Summary of cytotoxic activity of HA22-LR and HA22-LR-LO10 on various CD22$^+$ cells. A431 cells are a CD22$^-$ control. (*D*) Antitumor activity. Groups of five SCID mice bearing CA46 tumors were treated every other day × 3 (arrows), with 0.2% mouse serum albumin in PBS (◆), HA22-LR at 1.0 mg/kg (▲), HA22-LR-LO10 at 1.0 mg/kg (△), 3.0 mg/kg (○), or 5 mg/kg (□). *P < 0.05.

Cytotoxic Activity. The data in Fig. 5 *B* and *C* show that HA22-LR-LO10 is cytotoxic to CD22$^+$ lymphoma lines with IC$_{50}$s ranging from 0.3 to 1.6 ng/mL: it is 60% as active as HA22-LR on Daudi cells, 37% as active on Raji cells, and 32% as active on CA46 cells. Cytotoxicity is CD22-specific with no cytotoxic activity on CD22$^-$ A431 cells.

Antitumor Activity. The antitumor activity of HA22-LR-LO10 was evaluated in a mouse xenograft model in which CA46 cells were implanted subcutaneously (16). Treatment was begun on day 8, when the tumors reached about 150 mm^3. RITs were injected intravenously, every other day × 3, mimicking the schedule used to treat patients (4, 7). In mice that received 1.0 mg/kg HA22-LR (with no mutations in domain III), the tumors became smaller, reaching a nadir on day 16, and then began to regrow (Fig. 5*D*). An equal amount of HA22-LR-LO10 (1.0 mg/kg) appeared to have slightly more antitumor activity, even though it is somewhat less active against cultured CA46 cells. Because RITs without domain II are much less toxic to mice than HA22 that contains PE38 (17), we could give high doses without excess toxicity. Mice were treated with 3.0 or 5.0 mg/kg of HA22-LR-LO10 and on day 23 all had complete tumor regressions. On day 38 when the experiment was terminated, two of five mice treated at 3.0 mg/kg and four of five mice treated at 5.0 mg/kg still had complete regressions without signs of toxicity.

Pharmacokinetics. HA22-LR (molecular weight 50.5 kDa) is smaller than HA22 (molecular weight 63 kDa) and consequently has a shorter half-life in mice (15 vs. 8 min) (17). To assess the half-life of HA22-LR-LO10, BALB/c mice were injected with 10 μg of either HA22-LR or HA22-LR-LO10 and bled at intervals between 2 and 60 min. We measured the concentration of RIT in mice sera by ELISA (14, 17). Data were fit to a single exponential decay function. The half-lives were similar; the half-life of HA22-LR was 11.4 min ($r^2 = 0.92$), whereas the half-life of HA22-LR-LO10 was 9.8 min ($r^2 = 0.95$) (Fig. S1).

Antigenicity. We are unable to test the immunogenicity of HA22-LR-LO10 in humans so instead we assessed its antigenicity; that is, the binding of HA22-LR-LO10 to preexisting antibodies made against native RIT, as a surrogate measure of the immune response (9). We previously showed in mice that immunogenicity and antigenicity are closely related (13). We performed a competition assay in which we measured the concentration of RIT that reduced the level of patient serum antibodies reacting with HA22 by 50% (18).

Typical competition results from one patient are shown in Fig. 6*A*. HA22 (●) and HA22-LR (○) depleted the anti-PE antibodies from the anti-sera at low concentrations, whereas it required much higher concentrations of HA22-LR-LO10 (□) to partially deplete the anti-sera. HA22-LR-8M (△) had an intermediate effect. We analyzed sera from 25 patients treated with RITs SS1P, HA22, BL22, and LMB9. Fig. 6*B* shows that the binding of HA22-LR-LO10 was reduced more than 100-fold (100- to 10,000-fold) in 22 of 25 patients. As expected, antibody reactivity with HA22-LR and HA22-LR-8M was less than reactivity with HA22. However, HA22-LR-LO10 had even lower reactivity. Only sera from three patients did not show reduced reactivity with HA22-LR-LO10. We are in the process of identifying mutations that will reduce reactivity with the sera from these patients.

Discussion

We report here on the development of a unique RIT, HA22-LR-LO10, in which the major human-specific B-cell epitopes have been identified and removed or silenced. HA22-LR-LO10 has high cytotoxic activity and greatly reduced reactivity with human antisera containing neutralizing antibodies to the RITs now in
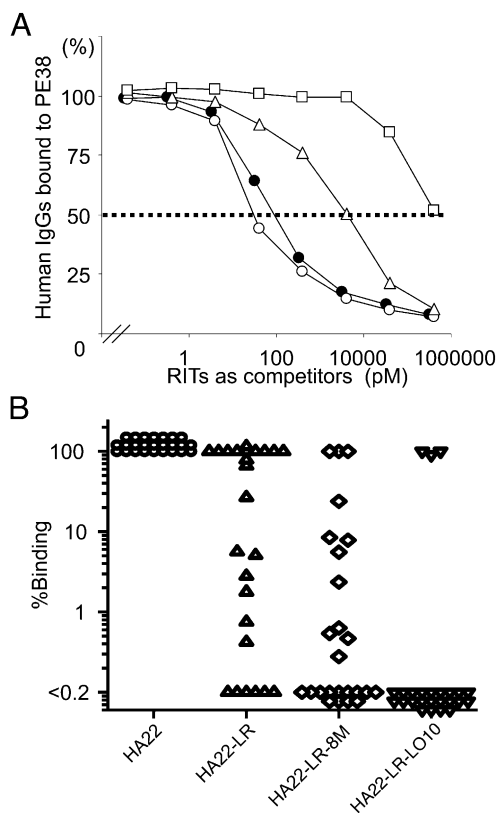
Fig. 6. The reactivity of HA22-LR-LO10 and various mutant RITs with human antisera. (*A*) A typical result showing displacement curves measuring the reactivity of native and mutant immunotoxins with patient serum. The concentration of HA22 (●), HA22-LR (○), HA22-LR-8M (△), and HA22-LR-LO10 (□) at which binding of antibodies to SS1P was inhibited by 50% (IC$_{50}$) is 85, 38, 3,610, and 396,000 pM, respectively. Using the IC$_{50}$ values we calculated the binding ratios as 223 for HA22-LR, 2.35 for HA22-LR-8M and < 0.0214% for HA22-LR-LO10. (*B*) Ratio of binding of mutant immunotoxins to binding of HA22 from 11 patients treated with BL22 (3), 1 with LMB9 (12), 7 with SS1P (7), and 6 with HA22 (4).

clinical trials. Based on previous studies in mice, HA22-LR-LO10 should also have low immunogenicity in humans.

Neutralizing antibody formation is a major impediment to the successful development of RIT therapy. The RITs that are currently in clinical trials (Moxetumomab pasudotox, SS1P, and LMB2) contain a 38-kDa fragment of PE made up of domains II and III (Fig. 1). Both domains II and III contain B-cell epitopes (13). The B-cell epitopes in domain II were removed when we found that all of domain II, except for the furin-processing site, could be excised without greatly diminishing the cytotoxic activity of the RIT (17). Our unique RIT (LR) contains only a 24-kDa catalytic fragment of PE (domain III). The B-cell epitopes in domain III were then silenced by converting large hydrophilic residues to alanine.

In previous studies we identified and removed mouse-specific B-cell epitopes by immunizing mice with RITs and isolating hybridomas that made mAbs to the immunotoxins (13). We used these mAbs to show that PE38 contained seven major epitopes, and identified their location on the protein surface through a series of point mutations (14). We adopted a different strategy in the present study, using M13 phage display to isolate human Fvs that react with the native toxin. We then used point mutations in RITs to locate B-cell epitopes reactive with these human Fvs. The data in Fig. 3 show that we identified six human B-cell epitopes in domain III using 41 Fvs. In the previous mouse study we used 24 mAbs to identify five epitopes in domain III (13).

Immunogenicity in humans can sometimes be predicted from studies in rodents and nonhuman primates, when the protein of interest is derived from a species such as bacteria, which is foreign to both humans and the other animal species evaluated. Atassi and Dolimbek used polyclonal antisera to compare the responses of humans and other animal species to peptides from Botulinum neurotoxin (19, 20). These authors observed that antisera from different animals often recognized similar regions on the antigen, but found there were boundary frame shifts and differences in immunodominance of specific regions among the antisera. Their study used polyclonal antisera for analyzing epitopes and only detected nonconformational epitopes. Our study is different because we detect conformational epitopes located on the surface of the native protein as it exists in the blood or other body fluids. Because we used individual Fvs for mapping, we were able to obtain detailed information on the composition and location of the epitopes. On the other hand, Fvs are monovalent, not bivalent as in antibodies, and the binding affinities are lower. Thus, we may have missed amino acids that contribute only weakly to an epitope.

Our hypothesis that B-cell epitopes are mainly comprised of bulky hydrophilic amino acids was confirmed by the results of this and the previous study (9). In both studies we were able to silence epitopes by mutating such residues to Ala. The location of these epitopes is shown in Fig. 4. In total, we identified 13 mutations that abrogated the binding of both human and mouse antibodies, 7 that were specific to humans and 8 that were mouse-specific.

Unexpectedly, we did not detect any human epitopes in the region of mouse epitope 7 at the C terminus of the protein, defined by residues K590 and Q592 (Fig. 3). We postulated that this observation might have been an experimental artifact resulting from the conjugation of the LMB9 RIT to biotin through lysine residues. An average of five biotin molecules were chemically conjugated to each RIT molecule, and an epitope containing K590 might have been blocked by conjugation to biotin. Therefore, we repeated the phage-enrichment studies (panning) with a RIT containing an average of two biotins/molecule. We still did not detect phage with Fvs reacting with that region of domain III. We expect that differences in the germ line repertoires of the human and mouse immune systems account for these differences.

To silence human epitopes and preserve cytotoxic activity, we began with HA22 containing mutations R467A and R490A, which are common to mouse and human and retain full cytotoxic activity. We then added additional mutations to remove or silence the remaining epitopes. The best mutant obtained was HA22-LR-LO10, which has a total of seven point mutations in domain III (Fig. 1). This mutant has high cytotoxic activity on cell lines with IC$_{50}$s ranging from 0.3 to 1.6 ng/mL (Fig. 5*C*), although it is somewhat less active than the parental molecule HA22-LR. In mice, however, HA22-LR-LO10 has comparable antitumor activity to HA22-LR (Fig. 5*D*). The rate of disappearance of the two proteins from the blood was similar, so pharmacokinetic differences cannot explain the unexpectedly high activity of HA22-LR-LO10. We postulate that HA22-LR-LO10 enters solid tumors more effectively than HA22 because it has fewer positively charged residues and has diminished interactions with negatively charged molecules in the matrix surrounding the tumor and tumor cells.

HA22-LR-LO10, like its predecessor HA22-LR, can be given in high doses to mice without observing excess toxicity. Many of the xenograft tumors shrank to an undetectable size after only three doses of the RIT (Fig. 5*D*). We predict that the effect would have been even more pronounced if additional doses had been administered. In summary, we have produced a unique RIT in which human B-cell epitopes have been identified and silenced, yet retain excellent cytotoxic and antitumor activity. We believe that this data supports further development of this agent for clinical trials.

Materials and Methods

scFv Phage Library. PAXgene tubes were used to extract RNA from blood samples of six patients who had made neutralizing antibodies to immunotoxins (PreAnalytiX/Qiagen) (Dataset S1). The scFv phage library was constructed as described previously; scFv fragments were digested with NcoI and NotI and subcloned into pCANTAB 5E (10, 11).

Phage Library Panning. LMB9 was biotinylated using EZ-Link sulfo–NHS-Biotin (Thermo Scientific), and the number of biotin groups on each LMB9–biotin was determined using the biotin quantitation kit (Thermo Scientific). Dynabead streptavidin-modified magnetic beads (Invitrogen) were preblocked in 3% BSA/PBST [0.1% (vol/vol) Tween-20]. To isolate phage that bound to PE38, the phage was incubated with LMB-9-biotin (10 µg for the first-round and 5 µg for subsequent rounds) in a total volume of 1 mL for 2 h at room temperature. Then, 2 mg of beads were added and incubated for 45 min. Bound and unbound phage were magnetically separated. Bound phage were released from beads with 1 mL of ice cold 0.1 M HCl for 10 min. The beads were magnetically separated, supernatants were transferred to a new tube, and the pH was neutralized with 200 µL Tris-HCl solution (pH 8.0). The eluted phage were rescued and panning was repeated twice using 10^{13} phage. After three rounds of panning, isolated single clones were tested for binding to antigen by ELISA using an anti-M13 mAb (GE Healthcare) as the detecting reagent. The DNA sequence of each clone was determined using BigDye Terminator v1.1 Cycle Sequencing Kit (Applied Biosystems). The sequences were aligned with the IMGT/V-Quest (www.imgt.org/IMGT_vquest/vquest). The affinity of isolated clones for LMB9 was measured and 56 high affinity clones were obtained. The clones binding to HA22-LR was measured, and 41 high affinity clones to domain III were obtained.

Competition ICC-ELISA. Competition ICC-ELISA was performed as previously described (9).

Amino Acid Sequence of Toxin in HA22-LR-LO10. AKASGGRHRQPRGWEQLPT-GAEFLGDGGDVSFSTRGTQNWTVERLLQAHAQLEERGYVFVGYHGTFLEAAQ SIV-FGGVRAA SQDLAAIWAG FYIAGDPALA YGYAQDQEPD AAGRIRNGAL LRVYV-PASSLPGFYRTSLTLAAPEAAGEVERLIGHPLPLALDAITGPEEE GGRLETILGWPLAE-RTVVIPSAIPTDPRNVGGDLDPSSIPDKEQAISALP DYASQPGKPP REDLK (first Ala is the final residue of the HA22 V_H).

Pharmacokinetics and Cytotoxic and Antitumor Activities. The pharmacokinetics and cytotoxic and antitumor activities were measured as previously described (13, 16, 21) using mAb IP12 for the blood levels. Animal experiments were performed under National Cancer Institute Animal Care and Use Committee-approved protocols.

Serum Antigenicity. Binding of HA22 or HA22 mutants to antibodies in human sera was measured in a displacement assay as previously described (9). Briefly, human sera were obtained under National Institutes of Health Institutional Review Board-approved protocols. Mesothelin-rFc was added to the ELISA plate (100 ng in 50 µL PBS/well) and incubated overnight at 4 °C (22). After washing, SS1P (antimesothelin Fv-PE38, 100 ng in 50 µL blocking buffer/well) was added for 1 h and bound to the mesothelin. In separate tubes, sera (97- to 30,658-fold dilutions) were mixed with 2 µg/mL of HA22 or HA22 mutants and incubated overnight at 4 °C. The SS1P containing plate was washed and followed by the addition of 50 µL of immunotoxin-antibody mixture to each well. Human antibodies that did not bind to HA22 or the HA22 mutants were captured by SS1P and quantified using HRP-conjugated rabbit anti-human IgG Fc (Jackson ImmunoRearch Laboratories), followed by a TMB substrate kit (Thermo Scientific). Binding curves were fit using a four-parameter logistic curve model by SoftMaxPro 4.0 (Molecular Devices). The IC_{50} values indicate the concentration of RIT that inhibit 50% of the antibody reactivity with SS1P.

Statistics. Mann–Whitney nonparametric methods was used: $P < 0.05$ was considered statistically significant.

1. Pastan I, Hassan R, Fitzgerald DJ, Kreitman RJ (2006) Immunotoxin therapy of cancer. *Nat Rev Cancer* 6:559–565.
2. FitzGerald DJ, Wayne AS, Kreitman RJ, Pastan I (2011) Treatment of hematologic malignancies with immunotoxins and antibody-drug conjugates. *Cancer Res* 71: 6300–6309.
3. Kreitman RJ, Pastan I (2011) Antibody fusion proteins: Anti-CD22 recombinant immunotoxin moxetumomab pasudotox. *Clin Cancer Res* 17:6398–6405.
4. Kreitman RJ, et al. (2012) Phase I trial of anti-CD22 recombinant immunotoxin moxetumomab pasudotox (CAT-8015 or HA22) in patients with hairy cell leukemia. *J Clin Oncol* 30:1822–1828.
5. Wayne AS, et al. (2010) Anti-CD22 immunotoxin RFB4(dsFv)-PE38 (BL22) for CD22-positive hematologic malignancies of childhood: Preclinical studies and phase I clinical trial. *Clin Cancer Res* 16:1894–1903.
6. Kreitman RJ, et al. (2000) Phase I trial of recombinant immunotoxin anti-Tac(Fv)-PE38 (LMB-2) in patients with hematologic malignancies. *J Clin Oncol* 18:1622–1636.
7. Hassan R, et al. (2007) Phase I study of SS1P, a recombinant anti-mesothelin immunotoxin given as a bolus I.V. infusion to patients with mesothelin-expressing mesothelioma, ovarian, and pancreatic cancers. *Clin Cancer Res* 13:5144–5149.
8. Kreitman RJ, Hassan R, Fitzgerald DJ, Pastan I (2009) Phase I trial of continuous infusion anti-mesothelin recombinant immunotoxin SS1P. *Clin Cancer Res* 15: 5274–5279.
9. Onda M, et al. (2011) Recombinant immunotoxin against B-cell malignancies with no immunogenicity in mice by removal of B-cell epitopes. *Proc Natl Acad Sci USA* 108: 5742–5747.
10. Marks JD, et al. (1991) By-passing immunization. Human antibodies from V-gene libraries displayed on phage. *J Mol Biol* 222:581–597.
11. Marks JD, Tristem M, Karpas A, Winter G (1991) Oligonucleotide primers for polymerase chain reaction amplification of human immunoglobulin variable genes and design of family-specific oligonucleotide probes. *Eur J Immunol* 21:985–991.
12. Benhar I, Reiter Y, Pai LH, Pastan I (1995) Administration of disulfide-stabilized Fv-immunotoxins B1(dsFv)-PE38 and B3(dsFv)-PE38 by continuous infusion increases their efficacy in curing large tumor xenografts in nude mice. *Int J Cancer* 62:351–355.
13. Onda M, et al. (2006) Characterization of the B cell epitopes associated with a truncated form of *Pseudomonas* exotoxin (PE38) used to make immunotoxins for the treatment of cancer patients. *J Immunol* 177:8822–8834.
14. Onda M, et al. (2008) An immunotoxin with greatly reduced immunogenicity by identification and removal of B cell epitopes. *Proc Natl Acad Sci USA* 105: 11311–11316.
15. Lee B, Richards FM (1971) The interpretation of protein structures: Estimation of static accessibility. *J Mol Biol* 55:379–400.
16. Kreitman RJ, Wang QC, FitzGerald DJP, Pastan I (1999) Complete regression of human B-cell lymphoma xenografts in mice treated with recombinant anti-CD22 immunotoxin RFB4(dsFv)-PE38 at doses tolerated by cynomolgus monkeys. *Int J Cancer* 81:148–155.
17. Weldon JE, et al. (2009) A protease-resistant immunotoxin against CD22 with greatly increased activity against CLL and diminished animal toxicity. *Blood* 113: 3792–3800.
18. Miller JJ, Valdes R (1992) Methods for calculating cross-reactivity in immunoassays. *J Clin Immunoassay* 15:97–107.
19. Atassi MZ, et al. (1996) Mapping of the antibody-binding regions on botulinum neurotoxin H-chain domain 855-1296 with antitoxin antibodies from three host species. *J Protein Chem* 15:691–700.
20. Atassi MZ, Dolimbek BZ (2004) Mapping of the antibody-binding regions on the HN-domain (residues 449-859) of botulinum neurotoxin A with antitoxin antibodies from four host species. Full profile of the continuous antigenic regions of the H-chain of botulinum neurotoxin A. *Protein J* 23:39–52.
21. Bang S, Nagata S, Onda M, Kreitman RJ, Pastan I (2005) HA22 (R490A) is a recombinant immunotoxin with increased antitumor activity without an increase in animal toxicity. *Clin Cancer Res* 11:1545–1550.
22. Onda M, et al. (2005) New monoclonal antibodies to mesothelin useful for immunohistochemistry, fluorescence-activated cell sorting, Western blotting, and ELISA. *Clin Cancer Res* 11:5840–5846.

MEDICAL SCIENCES